HHS Public Access

Author manuscript

Oncogene. Author manuscript; available in PMC 2017 April 07.

Published in final edited form as:

Oncogene. 2017 April 06; 36(14): 1925–1938. doi:10.1038/onc.2016.358.

ZEB1 Induces LOXL2-Mediated Collagen Stabilization and Deposition in the Extracellular Matrix to Drive Lung Cancer Invasion and Metastasis

David H. Peng[1,2], **Christin Ungewiss**[1,2], **Pan Tong**[3], **Lauren A. Byers**[1], **Jing Wang**[3], **Jaime Rodriguez Canales**[4], **Pamela A. Villalobos**[4], **Naohiro Uraoka**[4], **Barbara Mino**[4], **Carmen Behrens**[1], **Ignacio I. Wistuba**[4], **Richard I Han**[5], **Charles A. Wanna**[5], **Monica Fahrenholtz**[5], **Kathryn Jane Grande-Allen**[5], **Chad J. Creighton**[3,6], and **Don L. Gibbons**[1,7]

[1]Department of Thoracic/Head and Neck Medical Oncology, The University of Texas MD Anderson Cancer Center, Houston, TX 77030, USA

[2]The University of Texas Graduate School of Biomedical Sciences, Houston, TX 77030, USA

[3]Department of Bioinformatics and Computational Biology, The University of Texas MD Anderson Cancer Center, Houston, TX 77030, USA

[4]Department of Translational Molecular Pathology, The University of Texas MD Anderson Cancer Center, Houston, TX 77030, USA

[5]Department of Bioengineering, Rice University, Houston, TX 77005, USA

[6]Department of Medicine and Dan L. Duncan Cancer Center, Baylor College of Medicine, Houston, TX 77030, USA

[7]Department of Molecular and Cellular Oncology, The University of Texas MD Anderson Cancer Center, Houston, TX 77030, USA

Abstract

Lung cancer is the leading cause of cancer-related death, primarily due to distant metastatic disease. Metastatic lung cancer cells can undergo an epithelial-to-mesenchymal transition (EMT) regulated by many transcription factors, including double-negative feedback loop between the microRNA-200 (miR-200) family and ZEB1, but the precise mechanisms by which ZEB1-dependent EMT promotes malignancy remain largely undefined. While the cell-intrinsic effects of EMT are important for tumor progression, the reciprocal dynamic crosstalk between mesenchymal cancer cells and the extracellular matrix (ECM) is equally critical in regulating invasion and metastasis. Investigating the collaborative effect of EMT and ECM in the metastatic process

Corresponding Author: Dr. Don L. Gibbons, Department of Thoracic/Head and Neck Medical Oncology, The University of Texas MD Anderson Cancer Center, 1515 Holcombe Boulevard, Unit 432, Houston, TX 77030, USA, Phone: 713-792-9536, Fax: 713-792-1220, dlgibbon@mdanderson.org.

CONFLICT OF INTEREST

The authors declare no conflict of interest.

Supplementary Information accompanies the paper on the Oncogene website (http://www.nature.com/onc).

reveals increased collagen deposition in metastatic tumor tissues as a direct consequence of amplified collagen gene expression in ZEB1-activated mesenchymal lung cancer cells. Additionally, collagen fibers in metastatic lung tumors exhibit greater linearity and organization as a result of collagen crosslinking by the lysyl oxidase (LOX) family of enzymes. Expression of the LOX and LOXL2 isoforms is directly regulated by miR-200 and ZEB1, respectively, and their upregulation in metastatic tumors and mesenchymal cell lines is coordinated to that of collagen. Functionally, LOXL2, as opposed to LOX, is the principle isoform that crosslinks and stabilizes insoluble collagen deposition in tumor tissues. In turn, focal adhesion formation and FAK/SRC signaling is activated in mesenchymal tumor cells by crosslinked collagen in the ECM. Our study is the first to validate direct regulation of LOX and LOXL2 by the miR-200/ZEB1 axis, defines a novel mechanism driving tumor metastasis, delineates collagen as a prognostic marker, and identifies LOXL2 as a potential therapeutic target against tumor progression.

Keywords

EMT; ECM; LOXL2; lung cancer; metastasis

INTRODUCTION

Lung cancer is the leading cause of cancer-associated mortality largely due to metastatic disease (1), therefore understanding the molecular mechanisms governing metastasis is vital to improving overall patient survival. To that end, our group previously utilized the $Kras^{G12D};p53^{R172H}$ mouse model (KP) of metastatic lung adenocarcinoma to investigate this biological process (2). Studies with lung cancer cell lines derived from the tumor tissues of the KP model revealed an EMT-dependent mode of metastasis that is regulated by a double-negative feedback loop between the ZEB1 transcription factor and the microRNA-200 (miR-200) family (3–5). ZEB1 is a well-established master regulator of EMT in which increased expression of the transcription factor promotes a mesenchymal-like phenotype in cancer cells, resulting in greater invasive and metastatic activity (6, 7). Conversely, higher levels of miR-200 expression revert cells to a more epithelial state and abrogate metastasis (3, 8–11).

Despite the significance of miR-200 and ZEB1 in regulating EMT and metastasis, the specific downstream targets regulated by these two factors that produce the phenotypic changes are still largely undefined. While the cell-intrinsic effects of miR-200/ZEB1 are crucial in regulating EMT, findings by our group and others have demonstrated that tumor cell-extracellular matrix (ECM) interactions play a substantial role in regulating cell behavior, including EMT, invasion, and metastasis (3, 12–17). Several reports also suggest that there exists a reciprocal modulation between EMT and ECM structural and compositional properties that determines the invasiveness of cancer cells (18). A main component of the ECM that has been implicated in promoting EMT and driving cancer cell invasion is collagen, which represents the majority of interstitial ECM proteins in mammalian tissues (13, 16, 19). While collagen deposition appears to be necessary for tumor progression, numerous studies have shown that collagen requires enzymatic crosslinking to increase matrix stiffness and promote cancer cell invasion (3, 15, 20–23).

Lysyl oxidase (LOX) is one family of enzymes with a conserved catalytic region that has been known to crosslink collagen by oxidative deamination of its lysine residues and is developmentally necessary for insoluble collagen maturation and deposition in tissues (16, 24). Up-regulation of the LOX and LOXL2 isoforms has been shown to promote invasion and metastasis in certain cancer types (25). Despite ample evidence implicating LOX modification of the ECM in promoting breast tumor malignancy, there has been little work investigating this process in lung cancer systems. Moreover, the reciprocal crosstalk between EMT and the ECM in regulating lung cancer metastasis has yet to be revealed. A few reports have shown that lung adenocarcinomas possessing $Kras^{G12D};Lkb1^{-/-}$ mutations have increased LOX expression leading to metastasis while $Kras^{G12D};p53^{R172H}$ lung tumors do not show significant changes in LOX mRNA levels (26, 27). However, the studies do not address the fact that $Kras^{G12D};p53^{R172H}$ mice exhibit over twice the metastatic rate as the $Kras^{G12D};Lkb1^{L/L}$ mice (36.5% versus 16%) (2, 27), nor do they address the involvement of the EMT phenotype – shown to be adopted by a subset of cancer cells within the heterogeneous tumor tissue (3) – in metastasis. Additionally, these studies have solely focused on LOX without exploring the role of LOXL2, another major LOX isoform in ECM modification and metastasis.

Here, we demonstrate that mesenchymal lung cancer cells drive invasion and metastasis by increasing collagen deposition, crosslinking, and stabilization in their surrounding microenvironment due to an increase in ZEB1-regulated LOXL2 expression. We further demonstrate that collagen deposition in tumor tissues is necessary to activate focal adhesion signaling, which has been shown in our previous work to drive invasion and metastasis (17). We also define collagen type I and type III as promising prognostic markers and identify LOXL2 as a potential therapeutic target for the treatment of lung cancer.

RESULTS

Expression of collagen and ECM-associated genes correlates with EMT

To determine if EMT alters the expression of ECM-associated genes, we correlated gene expression patterns of patient tumor samples across multiple tumor types from the TCGA dataset to our previously reported 76-gene EMT signature score (28). The analysis revealed numerous ECM genes that have significant positive correlation with EMT ($r>0.5$) in at least six different epithelial tumor types (Figure 1A–B, Supplementary Figure 1A, and Supplementary Table S1). Focusing this analysis on lung adenocarcinoma and squamous cell carcinoma samples with a high correlation cutoff, we delineated multiple collagen family and ECM-associated genes that showed strong correlation with EMT (Figure 1B). To validate which specific collagen genes are differentially regulated by miR-200 and ZEB1, we performed qPCR assays of each collagen and collagen-associated gene from Figure 1B in a panel of human and murine epithelial and mesenchymal lung cancer cell lines with overexpression of ZEB1 or miR-200, respectively. Expression of miR-200 in mesenchymal murine and human lung cancer cells (H157 and 344SQ) consistently showed a decrease in mRNA levels for collagen type I, type III, as well as the collagen crosslinking enzymes LOX and LOXL2 (indicated by red arrows in Figure 1B, and Figure 1C – D). Conversely, ZEB1 expression in epithelial cells (H441 and 393P) consistently displayed an increase in mRNA

levels for these genes (Figure 1E and 1F). Further induction of EMT in the metastatic 344SQ murine lung cancer cell line by TGF-β (3) drastically up-regulated expression of the same collagen-associated genes as well. (Supplementary Figure S2E). This relationship between ECM-associated gene expression and EMT is consistent with results from 3D culture experiments, which demonstrate that Zeb1-mediated mesenchymal lung cancer cell invasion is not only dependent upon extrinsic collagen interaction (3) (Supplementary Figure S1B and S1C), but requires additional crosslinking, maturation, and deposition of collagen fibers when cultured under low collagen concentrations (12) (Supplementary Figure S1D). Although several other collagen genes were correlated with EMT, expression of these genes either showed inconsistent correlation between miR-200 and ZEB1 or had undetectable qPCR signals due to low basal levels of expression in the lung cancer cell lines tested (Supplementary Figure S2A–E).

Metastatic lung tumors have increased LOX, LOXL2, collagen deposition and linearization, correlating with their EMT status

Once we confirmed the correlation between EMT and collagen-associated gene expression *in vitro*, we next sought to verify this correlation *in vivo*. Analysis of primary lung tumors in KP mice capable of metastasis compared to non-metastatic $Kras^{G12D}$ mice revealed greater tumor areas presenting EMT patterns (based on Zeb1, E-cadherin, and Vimentin levels), which correlated with increased total collagen, collagen type I/type III deposition, and LOX/LOXL2 expression (Figure 2A). Second harmonics generation (SHG) microscopy of collagen fibers in the tumor tissues confirmed the increase in collagen density and revealed increased collagen fiber linearization in the KP tumors (Figure 2A). To validate that mesenchymal lung cancer cells were directly responsible for collagen deposition and fibrillar organization in primary tumors, we analyzed syngeneic tumors generated by subcutaneous injection of the non-metastatic 393P (epithelial) and highly metastatic 344SQ (mesenchymal) murine lung cancer cell lines in syngeneic wild type mice (3). Tissue stains confirmed the mesenchymal phenotype of 344SQ tumors (high nuclear Zeb1, low/mislocalized E-cadherin, and high cytoplasmic vimentin) compared to 393P tumors (low/absent nuclear Zeb1, high/membranous E-cadherin, absent vimentin), correlating with an increase in collagen type I, type III, and LOXL2 expression but no change in LOX levels (Figure 2B). SHG analysis also showed increased linear collagen fibers in the mesenchymal 344SQ tumors (Figure 2B). Previous studies have shown that the collagen fiber linearization is dependent on collagen crosslinking by LOX enzymes (12, 29, 30). Our findings suggest that up-regulation of collagen and LOX/LOXL2 in mesenchymal lung cancer cells results in increased collagen deposition and organization in the tumor microenvironment. Because secreted LOX and LOXL2 are potential therapeutic targets (25) that have been implicated as drivers of metastasis in various cancer types (22, 23, 29–31), we sought to further test their mechanistic role in metastasis.

LOX and LOXL2 are directly regulated by miR-200 and ZEB1, respectively

Since our previous studies have shown that the ZEB1/miR-200 axis is critical in regulating EMT and metastasis (3, 32), we wanted to determine if LOX and LOXL2 expression were regulated by this EMT program. We first evaluated the protein levels of LOX and LOXL2 in the panel of murine and human lung cancer cell lines that we previously characterized (3,

32–35) and observed higher levels of LOX and LOXL2 in mesenchymal cell lines with higher mesenchymal marker expression (Figure 3A, Supplementary Figure S3A, S3B, and S3C). Snail1 does not associate with the EMT status or LOX/LOXL2 expression in these cells, which is consistent with our previous findings (3, 32) that EMT in this system is Zeb1-dependent (Figure 3A). Although collagen I mRNA levels were higher in mesenchymal cells, collagen III expression did not significantly change between cell lines (Supplementary Figure S3A). Analyzing the conditioned media from our murine cell line panel revealed increased secreted LOXL2 protein from mesenchymal cells (Figure 3A) and demonstrated active LOXL2 enzymatic function by Amplex Red assays (36) (Figure 3B). Interestingly, we were unable to detect secreted LOX in the conditioned media from any of the cell lines (Figure 3A). Additional analysis of miR-200 and LOX/LOXL2 gene expression confirmed lower miR-200c levels in mesenchymal cell lines and showed a strong, inverse correlation to LOX and LOXL2 mRNA levels (Figure 3C). Forced expression of ZEB1 in epithelial murine and human cell lines induced EMT at the molecular level and led to an increase in LOX and LOXL2 protein levels (Figure 3C–D and Supplementary Figure S3D–F). Ectopic miR-200 expression or siRNA-mediated Zeb1 knockdown in mesenchymal cells had the contrasting effect (Figure 3D, Supplementary Figure S3D and S3G).

Due to the strong correlation between LOX, LOXL2, and the ZEB1/miR-200 axis, we proceeded to test whether these two enzymes were directly regulated by ZEB1 or miR-200. Evaluating potential microRNA binding sites in the 3′-untranslated region (UTR) of LOX using the TargetScan (www.targetscan.org) algorithm revealed one potential miR-200a and two potential miR-200b/c/429 seed sequences. Luciferase reporter assays with a cloned LOX 3′-UTR showed significant repression in luciferin signal in the presence of miR-200b/c but no repression with miR-200a (Figure 3E), which was further validated through introduction of miR-200b/c binding site mutations for each site individually or in combination. These findings were consistent with algorithm predictions that showed the first miR-200b site as having strong sequence binding while the miR-200a and second miR-200b sites had weaker complementation (Supplementary Figure S4A). Although LOXL2 has no predicted miR-200 binding sites, which we verified by 3′-UTR luciferase reporter assays (Supplementary Figure S4A and S4B), the promoter region contains several ZEB1 and ETS1 regulatory sites predicted by the JASPER transcription factor binding database (http://jaspar.genereg.net/). Luciferase reporter assays with the wild-type LOXL2 promoter region confirmed transcriptional regulation by ZEB1, which was verified by introduction of mutations into each of the ZEB1 binding sites individually and in combination. We further confirmed direct binding of ZEB1 to the endogenous LOXL2 promoter region by ZEB1 chromatin immunoprecipitation (ChIP) assays in multiple epithelial and mesenchymal cell lines (Figure 3F, Supplementary Figure S4C). The collagen I (COL1A1) and collagen III (COL3A1) genes did not show any predicted miR-200 binding sites in their 3′-UTR (Supplementary Figure S4A) nor any potential Zeb1 binding sites in their promoters (data not shown), suggesting an indirect mechanism of regulation.

LOX enzymatic function is necessary for lung cancer cell migration and invasion

We next wanted to assess the functional relevance of LOX and LOXL2 in promoting lung cancer cell migration and invasion. Inhibition of pan-LOX enzymatic activity with β-

aminopropionitrile (BAPN) significantly reduced enzymatic activity in conditioned media (Figure 4A) as well as Transwell migration and collagen invasion of mesenchymal murine 344SQ, 393P-ZEB1, and human H157 cells, but with no significant change in invasion through laminin-rich Matrigel (Figure 4B, Supplementary Figure S5A, and S5B). BAPN treatment of 393P-ZEB1 cells significantly reduced formation of invasive structures in 3D Matrigel/collagen I (Figure 4C) and reduced invasion of 344SQ cells through Matrigel alone upon TGF-β induction (Supplementary Figure S5C). Because LOX enzymes require copper as a co-factor, we also utilized the copper chelator D-Penicillamine (D-Pen) to inhibit LOX enzyme function and observed a significant reduction in 393P-ZEB1 2D migration/invasion in Transwell assays or 3D Matrigel/collagen I assays (Figure 4D and 4E). We observed no adverse effects of the inhibitors on cell proliferation and viability (Supplementary S5D and S5E). We next evaluated the effects of BAPN and D-Pen treatment on metastasis of 344SQ cells in syngeneic mice *in vivo*. Mice that received either inhibitor did not show a significant change in tumor size or metastatic lesions (Supplementary Figure S6A and S6B). Interestingly, analysis of collagen fibers by SHG revealed increased linearized collagen in primary tumor tissues (Supplementary Figure S6C), which suggests that the inhibitors either do not effectively reach the primary tumors or produced off-target effects. These results are consistent with several studies corroborating the inconsistency and ineffectiveness of chemical LOX inhibitors *in vivo* (25, 29, 37–40).

LOXL2 is necessary for collagen deposition, crosslinking and tumor cell metastasis

Given the inconsistent results with LOX chemical inhibitors *in vivo*, we next employed a genetic approach to study the role of LOX and LOXL2 in driving invasion and metastasis. Stable shRNA-mediated knockdown of LOX in metastatic 344SQ cells significantly decreased migration and invasion through Transwell Matrigel or collagen I chambers (Figure 5A), but did not have a significant effect on primary tumor growth or metastasis *in vivo* (Supplementary Figure S7A). In contrast, LOXL2 knockdown decreased invasion only through collagen I and significantly suppressed metastasis *in vivo* (Figure 5B and 5C). LOX and LOXL2 knockdown in a different metastatic KP cell line, 344LN, produced comparable results both *in vitro* and *in vivo*, with LOXL2 knockdown cells exhibiting diminished metastatic lung nodules that were also markedly smaller in size (Supplementary Figure S8A – S8D). Analysis of the conditioned media showed a significant decrease in enzymatic activity upon LOXL2 knockdown but an insignificant reduction when LOX was knocked down (Supplementary Figure S7B).

Developmentally, extracellular LOX enzymes are required for insoluble collagen deposition (16, 24, 41). Therefore, we analyzed the primary syngeneic tumors from our LOX and LOXL2 knockdown experiments for collagen deposition and reorganization. Upon LOXL2 knockdown, both collagen type I and type III deposition were significantly reduced, along with a significant decrease in linear collagen fibers (Figure 5D and 5E). Consistently, the decrease in tumor collagen content and organization was followed by a decrease in tissue stiffness (Figure 5F). In contrast, LOX knockdown had no effect on the deposition of either collagen isoform (Supplementary Figure S7C), which is consistent with results from our enzymatic activity assays. LOXL2 knockdown did not alter collagen I and III gene expression (Supplementary Figure S7D), which suggests that the decrease in collagen

deposition *in vivo* is due to lack of crosslinking and maturation. To further verify that LOXL2 is involved in collagen crosslinking and linearization, we visualized collagen fibers by scanning electron microscopy after culture of 344SQ-shLOXL2 cells in collagen I gels. Fiber alignment algorithms showed a significant reduction in average linear collagen fibers when LOXL2 was knocked down compared to the vector control (Figure 5G).

LOX and LOXL2 ectopic expression is not sufficient for epithelial cancer cell migration and invasion

Next, we took the converse approach and ectopically expressed LOX and LOXL2 in epithelial, non-metastatic 393P cells using a doxycycline-inducible pTRIPz vector. LOX and LOXL2 were either tagged or untagged with GFP at the N-terminus region. Western blots of LOX/LOXL2 induced cells confirmed proper expression of the desired proteins. However, only the untagged version of LOXL2 was detectable in the conditioned media, suggesting that the GFP interferes with the signaling peptide at the N-terminus region. GFP-tagged and untagged LOX was undetectable in the conditioned media (Supplementary Figure S9A and S9D). This finding was also verified by enzymatic assays of the conditioned media of the overexpression cell lines, which showed that only the LOXL2 expressing cells had extracellular enzymatic activity (Supplementary Figure S9B and S9E). There was no significant difference in Transwell migration and invasion with induced LOX expressed (Supplementary Figure S9C). However, when LOXL2 expression was induced, there was only a significant increase in invasion when extrinsic collagen was coated on the Transwell inserts (Supplementary Figure S9F). LOX and LOXL2 were also ectopically expressed in epithelial murine 307P and human H322 cells, which have low endogenous levels of LOX/LOXL2 (Figure 3A and Supplementary Figure S3B). Similar to 393P cells, we observed a significant, robust increase in invasion only through collagen coated Transwells when LOXL2 was expressed in 307P and H322 cells (Supplemetnary Figure S9G – J). Since collagen gene expression is unaltered when LOX or LOXL2 is overexpressed (Supplementary Figure S9K), this suggests that coordinate collagen expression by mesenchymal cells is also necessary to drive invasion and metastasis and that LOX or LOXL2 alone is not sufficient to promote migration and invasion.

LOXL2-mediated collagen deposition induces FAK/Src signaling *in vitro* and *in vivo*

Our group recently demonstrated that activation of the integrin β1/FAK/Src signaling pathway through collagen type I interaction is necessary for lung cancer invasion and metastasis (17). Since EMT causes lung cancer cells to deposit insoluble collagen by LOXL2 crosslinking, we investigated the potential autocrine effect that LOXL2 has on FAK/Src signaling. Immunofluorescent staining for activated phosphorylated FAK (Y861) and Src (Y416) showed that enzymatic inhibition or knockdown of LOXL2 decreased focal adhesion formation and FAK/Src signaling after TGF-β-mediated stimulation of 344SQ cells (Figure 6A – 6D). Western blotting confirmed the suppression of signaling by LOXL2 KD or inhibition and further emphasized that knockdown of LOX does not produce the same effect (Figure 6E). Further analysis of primary syngeneic tumors with LOXL2 knockdown (Figure 5D) by IHC staining revealed a decrease in activated FAK and Src versus control tumors (Figure 6F), correlating with the decrease in collagen type I and type III deposition in the tumors (Figure 5D). Collectively, our data supports a model in which ZEB1-driven

mesenchymal lung cancer cells deposit collagen in the tumor microenvironment through LOXL2 crosslinking, which further activates the integrin/FAK/Src signaling pathway in the cancer cells, leading to invasion and metastasis (Figure 6G).

Increased collagen, LOX, and LOXL2 expression predicts poor prognosis among patients with lung adenocarcinoma

Based upon these findings, we wanted to determine the prognostic value of the LOX and collagen proteins in predicting lung cancer patient survival and how their expression correlates with Zeb1 in human tumors. Pathologic assessment of stromal collagen I and III expression by IHC staining in a cohort of lung cancer specimens (n=490) revealed increased levels in lung adenocarcinoma (ACC) versus squamous cell carcinoma (SCC) samples (Figure 7A, 7B, and Supplementary Figure 10SA), but no statistically significant correlation to pathologic stage or patient outcome (Figure S10B and S10C). However, cytoplasmic scoring of collagen type I levels revealed greater amounts in poorly differentiated tumors of all histologic subtypes (Figure 7C), consistent with our findings correlating collagen expression with EMT. Although we observed a trend toward higher collagen levels in late-stage adenocarcinomas and in patients with poorer outcomes (Supplementary Figure S10D and S10E), the changes were statistically insignificant due to the relatively small sample size of late-stage tumors. Collagen type III did not display strong cytoplasmic staining in tumor tissues. To determine if Zeb1 correlated with collagen expression, we scored Zeb1 IHC stains specifically in the nuclei of tumor cells from the same cohort of tissue microarray specimens (Figure 7A). Although Zeb1 did not show a significant difference between tumor differentiation grades (Supplementary Figure S10F), there was an increase in expression in patients with SCC compared to ACC (Figure 7D). Zeb1 expression H-scores correlated moderately, but significantly with collagen I H-scores across all tumor histologic subtypes. However, when the samples were stratified by ACC and SCC histology, we observed an increased significant correlation between Zeb1 and collagen I expression in ACC patients (Figure 7F) but no significant correlation in patients with SCC (Supplementary Figure S10G). Zeb1 scores did not significantly correlate with stromal collagen I or III (Supplementary Figure S10H and S10I) nor did it correlate with patient outcome or pathological stage (data not shown).

Although we tested multiple antibodies for each, we were unable to analyze LOX and LOXL2 levels in the human specimens by IHC because none of the antibodies produced staining of clinically acceptable quality for scoring. To circumvent these issues, we performed Kaplan-Meier analyses using mRNA profiling from a large compendium of lung adenocarcinoma patients (n=1,586), which revealed decreased overall survival in patients whose tumors expressed elevated levels of collagen type I, type III, LOX, or LOXL2 (Figure 7D). This decrease in patient survival with high LOXL2 expression has also been previously observed in patients with lung SCC (42).

DISCUSSION

The underlying mechanisms governing metastasis remain largely undefined, with numerous studies proposing the Zeb1-driven EMT as a model for the dissemination process (3–8, 43–

45). In addition to the cancer cell-intrinsic changes induced by EMT, numerous studies have implicated the ECM as a crucial co-regulator of invasiveness (3, 12–15). Prior work by our group utilizing 3D culture systems demonstrates that a cell-inherent EMT is insufficient to produce invasion through laminin-rich Matrigel or synthetic gels of polyethylene glycol (15, 17). Lung cancer cells require additional extrinsic factors such as TGF-β stimulation (3) or collagen type I seeding in the matrix to drive the invasive phenotype (17), suggesting an undefined reciprocal dynamic interplay between the intracellular EMT machinery and the ECM. To elucidate the specific molecular alterations involved in the EMT-ECM crosstalk, we performed bioinformatic analyses of gene expression profiles from TCGA patient tumor samples and delineated a strong positive correlation between collagen-associated genes and EMT signatures. This observation is supported by histological and molecular analyses of lung tumor tissues and cell lines, which reveal that metastatic tumors have increased collagen levels due to direct deposition by mesenchymal cancer cells present in the heterogeneous tumor tissues. Our findings are the first to demonstrate that lung cancer cells that have undergone EMT are directly modifying the collagen composition of their surrounding microenvironment.

Concurrent with collagen expression patterns, we observed that the LOX and LOXL2 isoforms are up-regulated in metastatic lung tumor tissues and mesenchymal cell lines and our study is the first to demonstrate direct regulation of these targets by miR-200 and ZEB1. LOX proteins have been shown in several tumor types, most notably in breast cancer systems, to promote tumor progression and malignancy through various intracellular and extracellular mechanisms, including collagen fiber reorganization and crosslinking (12, 22, 23, 25, 30, 31, 46–52). Our functional studies confirm that LOXL2 is specifically driving *in vivo* metastatic disease while LOX may have an intracellular effect on the *in vitro* migratory ability of mesenchymal lung cancer cells. Interestingly, our biochemical and functional experiments also reveal that LOXL2, rather than LOX, is the major secreted isoform involved in collagen crosslinking and deposition in primary tumor tissues, consistent with the developmental role of LOX enzymes in maturing and stabilizing insoluble collagen in tissues (16, 24, 41). These results are in contrast with studies of other tumor types, which predominantly identify LOX as the primary isoform driving metastatic disease and matrix modification. Furthermore, although LOX knockdown decreases cell motility, ectopic LOX expression does not have the opposite effect, suggesting that another intracellular factor may work in tandem with LOX to promote migration and invasion. Similarly, LOXL2 overexpression alone has no effect on migration and invasion unless extrinsic collagen is introduced. Thus, LOXL2 is necessary, but not sufficient, to drive metastasis and emphasizes the complementary effects of EMT in driving ECM changes that potentiate the invasion/metastasis of mesenchymal cells. Our study is the first to determine the importance of LOXL2 in maintaining collagen type I and III deposition in primary tumor tissues for lung cancer metastasis.

The pleiotropic targets of the ZEB1/miR-200 axis in governing EMT and metastasis suggest multiple tiers of regulation throughout the dissemination process. We previously demonstrated that ZEB1/miR-200 regulates lung cancer cell invasion through CRKL recruitment of the integrin β1/FAK/Src signaling complex to focal adhesions in response to extracellular collagen (17). Here, we present a novel unifying mechanism by which

mesenchymal lung cancer cells modulate the compositional and structural properties of their surrounding ECM, resulting in stable collagen deposition in lung tumor tissues that activates FAK/Src signaling, producing invasion and metastasis. The Zeb1-induced amplification of collagen type I, type III, and LOXL2 gene expression correlates with decreased overall survival in lung cancer patients, conferring clinical significance of collagen as a prognostic marker and LOXL2 as a potential therapeutic target. Due to the off-target effects and toxicity of LOX chemical inhibitors as well as the isoform-specific role of LOXL2 in metastasis, utilizing a LOXL2 monoclonal antibody currently undergoing clinical trials shows greater promise for future therapeutic treatments of advanced lung cancer and metastatic disease (25, 29). Our findings also the pave way for future investigations delineating the invasion-promoting alterations of cancer cell signaling pathways in the presence of biochemically-modified collagen.

MATERIALS AND METHODS

Plasmids and Reagents

Mouse LOX shRNA constructs were purchased from Thermo Fisher Scientific (Cat#: RMM4534-EG16948, Grand Island, NY). Mouse LOXL2 shRNA constructs were cloned using primers listed in the Supplementary Methods into the pLKO.1 lentiviral vector. Murine LOX and LOXL2 isoforms were cloned using primers in Supplementary Methods and expressed using the Doxycycline inducible pTRIPz-GFP lentiviral vector. Viral vectors were the psPAX2 packaging and pMD2.G envelope vectors. Luciferase 3′-UTR reporter constructs were made by reverse-transcription PCR (RT-PCR) and PCR amplification of ~2.9 kb and ~2.6 kb of mouse LOX and LOXL2 3′-UTR mRNA, respectively. The promoter region for LOXL2 was PCR amplified from mouse genomic DNA ~1.3 kb upstream of the transcriptional start site. Site directed mutagenesis of binding sites were performed using the QuikChange II XL Site-Directed Mutagenesis Kit (Agilent, Santa Clara, CA, USA). Primers to clone all 3′-UTRs and LOXL2 promoter regions along with corresponding site-directed mutagenesis primers are listed in the Supplementary Methods.

Analysis of Human Cancer Datasets

Level 3 gene expression data from the TCGA pan-cancer data sets were used (53, 54). EMT score was calculated based on the EMT signature previously published (28, 33). Pearson correlation was used to quantify the association between EMT and collagen expression. To investigate if collagen family genes were enriched with strong correlations with EMT, we compared the correlations between EMT score and collagen family genes and correlations between EMT score and non-collagen family genes using the Kolmogorov–Smirnov test. For analysis of collagen-associated mRNA expression and lung cancer patient survival, we examined a previously-assembled compendium dataset (34) of 11 published expression profiling datasets for human lung adenocarcinomas (n = 1,492 tumors), with the addition of another dataset from Sato et al (55), patients represented in both Shedden and Chitale datasets (n=88 patients) were first removed from the Shedden dataset, and one patient from the Bild dataset thought to potentially represent SQCC was also removed (leaving n = 1,586 tumors in total).

Cell Culture and Transfections

All lung cancer cell lines were cultured in RPMI 1640 supplemented with 10% fetal bovine serum (FBS). HEK-293 cells were cultured in DMEM supplemented with 10% FBS. Lentiviral vectors were co-transfected in HEK-293 cell with Lipofectamine LTX (Thermo). Luciferase reporter assays used Lipofectamine 2000 (Thermo) as the transfection reagent. Murine cell lines were previously generated by our lab (3) and human cell lines were obtained through ATCC. All cell lines were verified to by mycoplasma negative monthly.

QPCR and Western Blotting

Total RNA was isolated from cells by TRIzol (Thermo) according to manufacturer protocol and cDNA was generated using iSCRIPT reagents (Bio-Rad, Hercules, CA). QPCR assays were performed using SYBR Green PCR Master Mix (Thermo) along with primers listed in the Supplementary Methods and normalized to the L32 gene. Cell lysates were prepared according to the RIPA buffer protocol (CS9806), separated by SDS-PAGE, transferred to nitrocellulose membranes, and probed with antibodies listed in the Supplementary Methods.

Luciferase Reporter Assays

Luciferase reporter assays were carried out by transfection of 500 ng of the reporter constructs in specified cell lines with 50 nM miR-200a/b/c precursors where appropriate (Thermo). Assays were carried out using Dual-Luciferase Reporter Assay kit (Promega, Madison, WI).

Chromatin Immunoprecipitation Assays

Chromatin immunoprecipitation assays were performed as previously described (32, 35). Immunoprecipitation was carried out using an anti-ZEB1 antibody or mock IgG control (Santa Cruz, Dallas, TX). Promoter segment enrichment was analyzed by qPCR using primers (Supplementary methods) flanking the potential ZEB1 binding sites along the LOXL2 promoter.

Migration and Invasion Assays

Migration/invasion assays were performed using 8 μm Transwell inserts pre-coated with Matrigel or 100 μl of 0.2 mg/ml collagen type I (BD Biosciences, San Jose, CA). Assays progressed at 37°C for 8 hrs for human cell lines and 20 hrs for murine cell lines following a published protocol (3). BAPN and D-Penicillamine were purchased from Sigma (St. Louis, MO). Inserts were stained with crystal violet and cells were imaged by bright field microscopy and counted using ImageJ software.

3D Matrigel and Matrigel/Collagen Culture

Glass 8-well chamber slides (Thermo) were coated with 100 μl Matrigel or Matrigel/collagen type I mix at 1.5 mg/ml final collagen concentration. Cells were seeded in the matrices and cultured for 7 days with indicated daily treatments. Collagen gels for SEM analysis were 2 mg/ml of pure collagen with cells encapsulated and treated with TGF-β for 7 days.

Syngeneic In Vivo Tumorigenesis and Metastasis Assays

Cells were subcutaneously injected in the right flanks of male, syngeneic 129/sv mice at 3 months of age and allowed to form tumors for 5 to 6 weeks. After euthanasia, tumors were measured and lung metastatic nodules were quantified. For *in vivo* inhibitor treatments, mice received 100 mg/kg BAPN or 150 mg/kg D-Pen in H_2O or PBS, respectively, by daily intraperitoneal injection. Lung tissues and primary tumor tissues were formalin fixed, paraffin embedded, and sectioned for further analysis. All animal experiments were reviewed and approved by the Institutional Animal Care and Use Committee at The University of Texas MD Anderson Cancer Center.

Immunohistochemistry (IHC) and Second Harmonics Generation (SHG) Microscopy

Paraffin embedded tissue sections were rehydrated, blocked with goat serum, and probed with antibodies listed in the Supplementary Methods. Tissues were subsequently washed and probed with HRP-conjugated secondary antibodies and signal was attained by developing with a DAB reagent. For SHG microscopy, tissues stained by H&E were visualized using a Zeiss LSM 7 MP Multiphoton Microscope at an excitation wavelength of 800 nm and collagen fiber signals were detected at 380–430 nm using bandpass filters. Collagen linearity was calculated as a ratio of the total length versus the end-to-end length of the individual collagen fiber as previously described (12).

Immunofluorescence (IF) Staining

IF stains were performed as previously described (17), stained with antibodies listed in the Supplementary Methods, and visualized by fluorescence microscopy.

Proliferation Assay

Cells were seeded in 96-well plates at 500 cells/well and treated with BAPN or D-Pen at specified concentrations. Proliferation was measured following the WST-1 (Roche, Basel, Switzerland) protocol and absorbance was measured at 450 nm after 2 hours.

Amplex Red Assay

LOX family enzyme activity from cell culture media with indicated treatments was measured using the Amplex Red protocol (Thermo) and 2mM benzylamine (Sigma).

Mechanical Testing

A bioindenter (BHT, Anton Paar, Ashland, VA) was used to test the local mechanical properties of tumor tissues approximately 1 cm wide under hydrated conditions and carried out using a 500 μm diameter flat punch indentation tip with a constant loading rate up to a maximum load of 60 μN. Instrumentation software analysis of the resulting unloading curve by the Oliver & Pharr method was used to calculate the indentation modulus (56).

Cell macerated scanning electron microscopy

A modification of the NaOH cell-maceration technique reported by Rossi was used (57). This technique dissolves the cellular elements, fixed, and dehydrated, leaving behind the collagen matrix, network, allowing three-dimensional imaging using SEM. Dehydrated

specimens were critical point dried (Critical Point Dyer 850, Electron Microscopy Science, Hatfield, PA), mounted on aluminum mount (Electron Microscopy Science, Hatfield, PA), sputter coated with 15 nm gold palladium in a Denton Desk V sputter (Moorestown, NJ), and viewed in a FEI Quanta 400 ESEM FEG (Hillsboro, Oregon).

Collagen Fiber Alignment Analysis

A custom-written MATLAB program was used to analyze the alignment of the collagen fibers within the SEM images. The program imported the SEM .tiff files, enhanced the grayscale contrast, applied a filter and a mask to reduce white noise and detect the fiber edges, respectively (58). The program then developed a high-resolution histogram (with 0.5 degree bins) of the fiber directions and set the mean fiber direction at 0 degrees. After preparing this histogram for each SEM image, the distributions from multiple pictures taken from each gel were compiled to obtain an accurate representation of the alignment of each gel. The compiled histogram data from each gel was averaged across all gels within a treatment group and then fit to a normal distribution. Because the compiled data sets were extremely large, before performing a statistical analysis the data was subsampled to retain only one out of every hundred points within each 0.5 degree bin.

Statistics

Statistical analysis was performed with unpaired student's t-test or otherwise stated.

Supplementary Material

Refer to Web version on PubMed Central for supplementary material.

Acknowledgments

We thank Dr. G. Goodall (University of Adelaide, Australia) for the kind gift of the pTRIPz-miR-200 expression constructs. We thank Dr. M. Dickinson (Baylor College of Medicine, Houston, TX, USA) for providing access to the multiphoton microscope for SHG analysis. We would like to thank members of the Gibbons lab for their assistance and critical reading of the manuscript. This work was supported by NCI K08 CA151661 (DLG), an MD Anderson Cancer Center Physician Scientist Award (DLG), Rexanna's Foundation for Fighting Lung Cancer (DLG), and CPRIT grant RP120713 P2 (DLG & JGA). DP was supported by a CPRIT Graduate Scholar Training Grant (RP140106). JW and PT are supported by Lung SPORE (P50 CA070907), Cancer Center Support Grant (CCSG CA016672), and Mary K. Chapman Foundation. CJC was supported by CPRIT grant RP120713 C2 and NCI grant CA125123. LAB and DLG are R. Lee Clark Fellows of the University of Texas MD Anderson Cancer Center, supported by the Jeane F. Shelby Scholarship Fund.

References

1. Siegel R, Ma J, Zou Z, Jemal A. Cancer statistics, 2014. CA Cancer J Clin. 2014; 64(1):9–29. [PubMed: 24399786]
2. Gibbons DL, Lin W, Creighton CJ, Zheng S, Berel D, Yang Y, et al. Expression signatures of metastatic capacity in a genetic mouse model of lung adenocarcinoma. PLoS One. 2009; 4(4):e5401. [PubMed: 19404390]
3. Gibbons DL, Lin W, Creighton CJ, Rizvi ZH, Gregory PA, Goodall GJ, et al. Contextual extracellular cues promote tumor cell EMT and metastasis by regulating miR-200 family expression. Genes Dev. 2009; 23(18):2140–51. [PubMed: 19759262]
4. Gregory PA, Bert AG, Paterson EL, Barry SC, Tsykin A, Farshid G, et al. The miR-200 family and miR-205 regulate epithelial to mesenchymal transition by targeting ZEB1 and SIP1. Nat Cell Biol. 2008; 10(5):593–601. [PubMed: 18376396]

5. Gregory PA, Bracken CP, Smith E, Bert AG, Wright JA, Roslan S, et al. An autocrine TGF-beta/ZEB/miR-200 signaling network regulates establishment and maintenance of epithelial-mesenchymal transition. Mol Biol Cell. 2011; 22(10):1686–98. [PubMed: 21411626]
6. Yang J, Weinberg RA. Epithelial-mesenchymal transition: at the crossroads of development and tumor metastasis. Developmental cell. 2008; 14(6):818–29. [PubMed: 18539112]
7. Wellner U, Schubert J, Burk UC, Schmalhofer O, Zhu F, Sonntag A, et al. The EMT-activator ZEB1 promotes tumorigenicity by repressing stemness-inhibiting microRNAs. Nat Cell Biol. 2009; 11(12):1487–95. [PubMed: 19935649]
8. Ma L, Weinberg RA. Micromanagers of malignancy: role of microRNAs in regulating metastasis. Trends Genet. 2008; 24(9):448–56. [PubMed: 18674843]
9. Davalos V, Moutinho C, Villanueva A, Boque R, Silva P, Carneiro F, et al. Dynamic epigenetic regulation of the microRNA-200 family mediates epithelial and mesenchymal transitions in human tumorigenesis. Oncogene. 2012; 31(16):2062–74. [PubMed: 21874049]
10. Kundu ST, Byers LA, Peng DH, Roybal JD, Diao L, Wang J, et al. The miR-200 family and the miR-183~96~182 cluster target Foxf2 to inhibit invasion and metastasis in lung cancers. Oncogene. 2015
11. Roybal JD, Zang Y, Ahn YH, Yang Y, Gibbons DL, Baird BN, et al. miR-200 Inhibits lung adenocarcinoma cell invasion and metastasis by targeting Flt1/VEGFR1. Mol Cancer Res. 2011; 9(1):25–35. [PubMed: 21115742]
12. Levental KR, Yu H, Kass L, Lakins JN, Egeblad M, Erler JT, et al. Matrix crosslinking forces tumor progression by enhancing integrin signaling. Cell. 2009; 139(5):891–906. [PubMed: 19931152]
13. Egeblad M, Rasch MG, Weaver VM. Dynamic interplay between the collagen scaffold and tumor evolution. Curr Opin Cell Biol. 2010; 22(5):697–706. [PubMed: 20822891]
14. Streuli CH, Bailey N, Bissell MJ. Control of Mammary Epithelial Differentiation - Basement-Membrane Induces Tissue-Specific Gene-Expression in the Absence of Cell Cell-Interaction and Morphological Polarity. J Cell Biol. 1991; 115(5):1383–95. [PubMed: 1955479]
15. Gill BJ, Gibbons DL, Roudsari LC, Saik JE, Rizvi ZH, Roybal JD, et al. A synthetic matrix with independently tunable biochemistry and mechanical properties to study epithelial morphogenesis and EMT in a lung adenocarcinoma model. Cancer Res. 2012; 72(22):6013–23. [PubMed: 22952217]
16. Gilkes DM, Semenza GL, Wirtz D. Hypoxia and the extracellular matrix: drivers of tumour metastasis. Nat Rev Cancer. 2014; 14(6):430–9. [PubMed: 24827502]
17. Ungewiss C, Rizvi ZH, Roybal JD, Peng DH, Gold KA, Shin DH, et al. The microRNA-200/Zeb1 axis regulates ECM-dependent beta1-integrin/FAK signaling, cancer cell invasion and metastasis through CRKL. Sci Rep. 2016; 6:18652. [PubMed: 26728244]
18. Jung HY, Fattet L, Yang J. Molecular pathways: linking tumor microenvironment to epithelial-mesenchymal transition in metastasis. Clin Cancer Res. 2015; 21(5):962–8. [PubMed: 25107915]
19. Shintani Y, Maeda M, Chaika N, Johnson KR, Wheelock MJ. Collagen I promotes epithelial-to-mesenchymal transition in lung cancer cells via transforming growth factor-beta signaling. American journal of respiratory cell and molecular biology. 2008; 38(1):95–104. [PubMed: 17673689]
20. Leight JL, Wozniak MA, Chen S, Lynch ML, Chen CS. Matrix rigidity regulates a switch between TGF-beta1-induced apoptosis and epithelial-mesenchymal transition. Mol Biol Cell. 2012; 23(5): 781–91. [PubMed: 22238361]
21. Paszek MJ, Zahir N, Johnson KR, Lakins JN, Rozenberg GI, Gefen A, et al. Tensional homeostasis and the malignant phenotype. Cancer Cell. 2005; 8(3):241–54. [PubMed: 16169468]
22. Erler JT, Bennewith KL, Nicolau M, Dornhofer N, Kong C, Le QT, et al. Lysyl oxidase is essential for hypoxia-induced metastasis. Nature. 2006; 440(7088):1222–6. [PubMed: 16642001]
23. Cox TR, Bird D, Baker AM, Barker HE, Ho MW, Lang G, et al. LOX-mediated collagen crosslinking is responsible for fibrosis-enhanced metastasis. Cancer Res. 2013; 73(6):1721–32. [PubMed: 23345161]
24. Kagan HM, Li W. Lysyl oxidase: properties, specificity, and biological roles inside and outside of the cell. J Cell Biochem. 2003; 88(4):660–72. [PubMed: 12577300]

25. Barker HE, Cox TR, Erler JT. The rationale for targeting the LOX family in cancer. Nat Rev Cancer. 2012; 12(8):540–52. [PubMed: 22810810]
26. Gao Y, Xiao Q, Ma H, Li L, Liu J, Feng Y, et al. LKB1 inhibits lung cancer progression through lysyl oxidase and extracellular matrix remodeling. Proc Natl Acad Sci U S A. 2010; 107(44): 18892–7. [PubMed: 20956321]
27. Han X, Li F, Fang Z, Gao Y, Li F, Fang R, et al. Transdifferentiation of lung adenocarcinoma in mice with Lkb1 deficiency to squamous cell carcinoma. Nat Commun. 2014; 5:3261. [PubMed: 24531128]
28. Byers LA, Diao L, Wang J, Saintigny P, Girard L, Peyton M, et al. An epithelial-mesenchymal transition gene signature predicts resistance to EGFR and PI3K inhibitors and identifies Axl as a therapeutic target for overcoming EGFR inhibitor resistance. Clin Cancer Res. 2013; 19(1):279–90. [PubMed: 23091115]
29. Barry-Hamilton V, Spangler R, Marshall D, McCauley S, Rodriguez HM, Oyasu M, et al. Allosteric inhibition of lysyl oxidase-like-2 impedes the development of a pathologic microenvironment. Nat Med. 2010; 16(9):1009–17. [PubMed: 20818376]
30. Pickup MW, Laklai H, Acerbi I, Owens P, Gorska AE, Chytil A, et al. Stromally derived lysyl oxidase promotes metastasis of transforming growth factor-beta-deficient mouse mammary carcinomas. Cancer Res. 2013; 73(17):5336–46. [PubMed: 23856251]
31. Peng L, Ran YL, Hu H, Yu L, Liu Q, Zhou Z, et al. Secreted LOXL2 is a novel therapeutic target that promotes gastric cancer metastasis via the Src/FAK pathway. Carcinogenesis. 2009; 30(10): 1660–9. [PubMed: 19625348]
32. Ahn YH, Gibbons DL, Chakravarti D, Creighton CJ, Rizvi ZH, Adams HP, et al. ZEB1 drives prometastatic actin cytoskeletal remodeling by downregulating miR-34a expression. J Clin Invest. 2012; 122(9):3170–83. [PubMed: 22850877]
33. Chen L, Gibbons DL, Goswami S, Cortez MA, Ahn YH, Byers LA, et al. Metastasis is regulated via microRNA-200/ZEB1 axis control of tumour cell PD-L1 expression and intratumoral immunosuppression. Nat Commun. 2014; 5:5241. [PubMed: 25348003]
34. Yang Y, Ahn YH, Chen Y, Tan X, Guo L, Gibbons DL, et al. ZEB1 sensitizes lung adenocarcinoma to metastasis suppression by PI3K antagonism. J Clin Invest. 2014; 124(6):2696–708. [PubMed: 24762440]
35. Yang Y, Ahn YH, Gibbons DL, Zang Y, Lin W, Thilaganathan N, et al. The Notch ligand Jagged2 promotes lung adenocarcinoma metastasis through a miR-200-dependent pathway in mice. J Clin Invest. 2011; 121(4):1373–85. [PubMed: 21403400]
36. Palamakumbura AH, Trackman PC. A fluorometric assay for detection of lysyl oxidase enzyme activity in biological samples. Anal Biochem. 2002; 300(2):245–51. [PubMed: 11779117]
37. Vadasz Z, Kessler O, Akiri G, Gengrinovitch S, Kagan HM, Baruch Y, et al. Abnormal deposition of collagen around hepatocytes in Wilson's disease is associated with hepatocyte specific expression of lysyl oxidase and lysyl oxidase like protein-2. J Hepatol. 2005; 43(3):499–507. [PubMed: 16023247]
38. Hollosi P, Yakushiji JK, Fong KS, Csiszar K, Fong SF. Lysyl oxidase-like 2 promotes migration in noninvasive breast cancer cells but not in normal breast epithelial cells. Int J Cancer. 2009; 125(2): 318–27. [PubMed: 19330836]
39. Zhan P, Shen XK, Qian Q, Zhu JP, Zhang Y, Xie HY, et al. Down-regulation of lysyl oxidase-like 2 (LOXL2) is associated with disease progression in lung adenocarcinomas. Med Oncol. 2012; 29(2):648–55. [PubMed: 21519871]
40. Payne SL, Hendrix MJ, Kirschmann DA. Paradoxical roles for lysyl oxidases in cancer–a prospect. J Cell Biochem. 2007; 101(6):1338–54. [PubMed: 17471532]
41. Hong HH, Pischon N, Santana RB, Palamakumbura AH, Chase HB, Gantz D, et al. A role for lysyl oxidase regulation in the control of normal collagen deposition in differentiating osteoblast cultures. J Cell Physiol. 2004; 200(1):53–62. [PubMed: 15137057]
42. Peinado H, Moreno-Bueno G, Hardisson D, Perez-Gomez E, Santos V, Mendiola M, et al. Lysyl oxidase-like 2 as a new poor prognosis marker of squamous cell carcinomas. Cancer Res. 2008; 68(12):4541–50. [PubMed: 18559498]

43. Kalluri R, Weinberg RA. The basics of epithelial-mesenchymal transition. J Clin Invest. 2009; 119(6):1420–8. [PubMed: 19487818]
44. Alderton GK. Metastasis: Epithelial to mesenchymal and back again. Nat Rev Cancer. 2013; 13(1): 3. [PubMed: 23258155]
45. Xiao D, He J. Epithelial mesenchymal transition and lung cancer. J Thorac Dis. 2010; 2(3):154–9. [PubMed: 22263037]
46. Baker AM, Cox TR, Bird D, Lang G, Murray GI, Sun XF, et al. The role of lysyl oxidase in SRC-dependent proliferation and metastasis of colorectal cancer. J Natl Cancer Inst. 2011; 103(5):407–24. [PubMed: 21282564]
47. Barker HE, Bird D, Lang G, Erler JT. Tumor-secreted LOXL2 activates fibroblasts through FAK signaling. Mol Cancer Res. 2013; 11(11):1425–36. [PubMed: 24008674]
48. Barker HE, Chang J, Cox TR, Lang G, Bird D, Nicolau M, et al. LOXL2-mediated matrix remodeling in metastasis and mammary gland involution. Cancer Res. 2011; 71(5):1561–72. [PubMed: 21233336]
49. Fong SF, Dietzsch E, Fong KS, Hollosi P, Asuncion L, He Q, et al. Lysyl oxidase-like 2 expression is increased in colon and esophageal tumors and associated with less differentiated colon tumors. Genes Chromosomes Cancer. 2007; 46(7):644–55. [PubMed: 17394133]
50. Lucero HA, Kagan HM. Lysyl oxidase: an oxidative enzyme and effector of cell function. Cell Mol Life Sci. 2006; 63(19–20):2304–16. [PubMed: 16909208]
51. Canesin G, Cuevas EP, Santos V, Lopez-Menendez C, Moreno-Bueno G, Huang Y, et al. Lysyl oxidase-like 2 (LOXL2) and E47 EMT factor: novel partners in E-cadherin repression and early metastasis colonization. Oncogene. 2015; 34(8):951–64. [PubMed: 24632622]
52. Peinado H, Del Carmen Iglesias-de la Cruz M, Olmeda D, Csiszar K, Fong KS, Vega S, et al. A molecular role for lysyl oxidase-like 2 enzyme in snail regulation and tumor progression. EMBO J. 2005; 24(19):3446–58. [PubMed: 16096638]
53. Akbani R, Ng PK, Werner HM, Shahmoradgoli M, Zhang F, Ju Z, et al. A pan-cancer proteomic perspective on The Cancer Genome Atlas. Nat Commun. 2014; 5:3887. [PubMed: 24871328]
54. Hoadley KA, Yau C, Wolf DM, Cherniack AD, Tamborero D, Ng S, et al. Multiplatform analysis of 12 cancer types reveals molecular classification within and across tissues of origin. Cell. 2014; 158(4):929–44. [PubMed: 25109877]
55. Sato M, Larsen JE, Lee W, Sun H, Shames DS, Dalvi MP, et al. Human lung epithelial cells progressed to malignancy through specific oncogenic manipulations. Mol Cancer Res. 2013; 11(6):638–50. [PubMed: 23449933]
56. Oliver WC, Pharr GM. An Improved Technique for Determining Hardness and Elastic-Modulus Using Load and Displacement Sensing Indentation Experiments. J Mater Res. 1992; 7(6):1564–83.
57. Rossi MA, Abreu MA, Santoro LB. Connective Tissue Skeleton of the Human Heart: A Demonstration by Cell-Maceration Scanning Electron Microscope Method. Circulation. 1998; 97(9):934–5. [PubMed: 9521343]
58. Chaudhuri BB, Kundu P, Sarkar N. Detection and Gradation of Oriented Texture. Pattern Recogn Lett. 1993; 14(2):147–53.

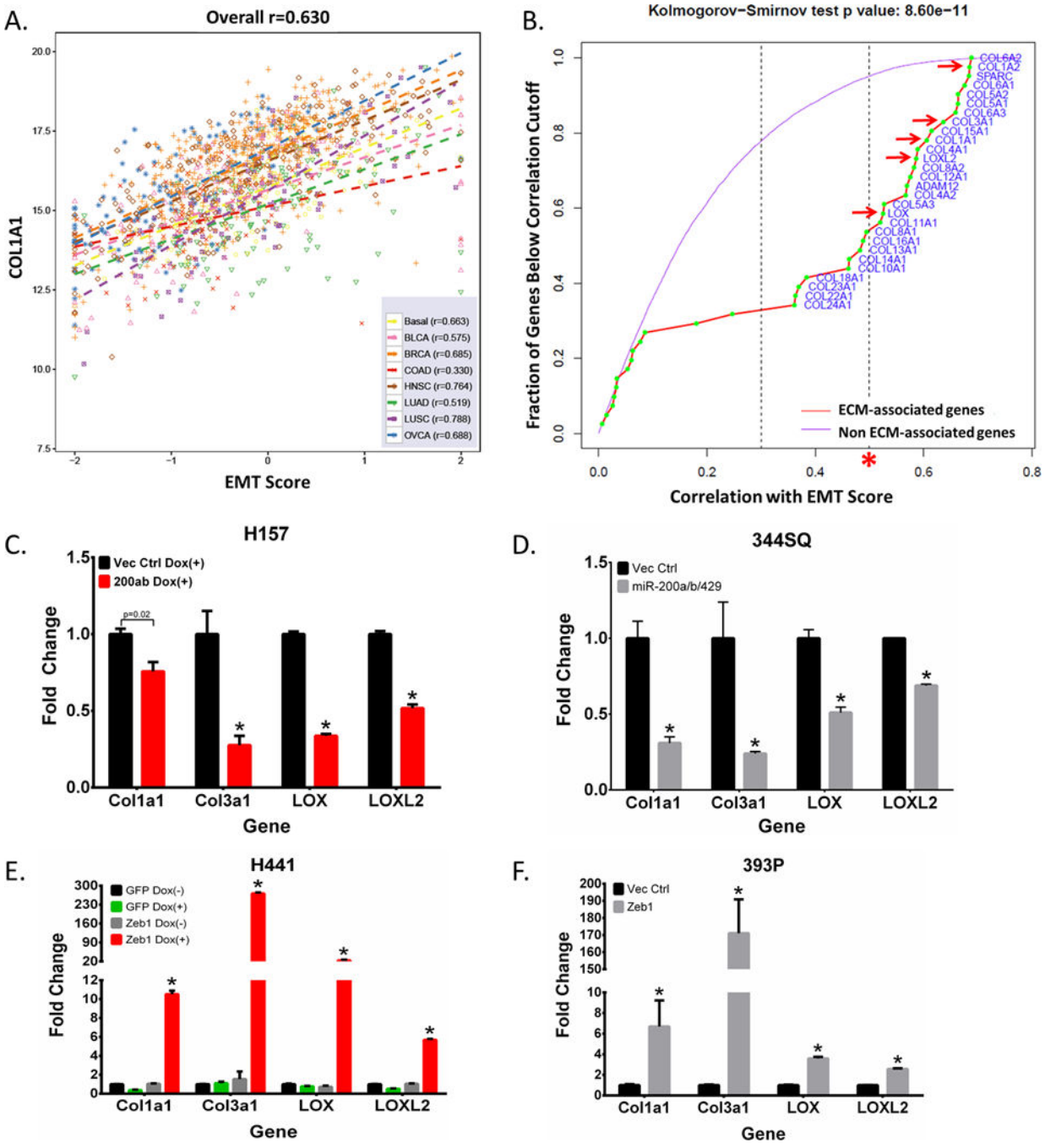

Figure 1. Expression of collagen and ECM-associated genes correlates with EMT

(A) Representative plot correlating gene expression of collagen 1A1 to EMT scores of human tumors from TCGA datasets (BASAL: Basal-like breast cancer; BCLA: Bladder Urothelial Carcinoma; BRCA: Breast invasive carcinoma; COAD: Colon adenocarcinoma; HNSC: Head and Neck squamous cell carcinoma; LUAD: Lung adenocarcinoma; LUSC: Lung squamous cell carcinoma; OVCA: Ovarian carcinoma). **(B)** Graph showing the fraction of genes from TCGA dataset analysis below the correlation value to EMT score. Purple line represents genes that are not associated with the ECM but still correlated with

EMT gene signatures. ECM-related genes are represented by the red line with collagen-associated genes specifically denoted by green points. Collagen genes above a high correlation cutoff ($r>0.5$), as indicated by the red asterisks, were selected for further validation. Red arrows indicate qPCR validated collagen-associated genes that were consistently downregulated by miR-200, upregulated by Zeb1, and selected for further analyses. **(C, D)** qPCR analysis for relative expression of COL1A1, COL3A1, LOX, and LOXL2 in human H157 and murine 344SQ mesenchymal lung cancer cell lines with inducible and stable miR-200 expression, respectively. **(E, F)** qPCR analysis for relative expression of COL1A1, COL3A1, LOX, and LOXL2 in human H441 and murine 393P epithelial lung cancer cell lines with inducible and stable Zeb1 expression, respectively. Asterisks (*) for qPCR data indicate significance value of $p<0.01$.

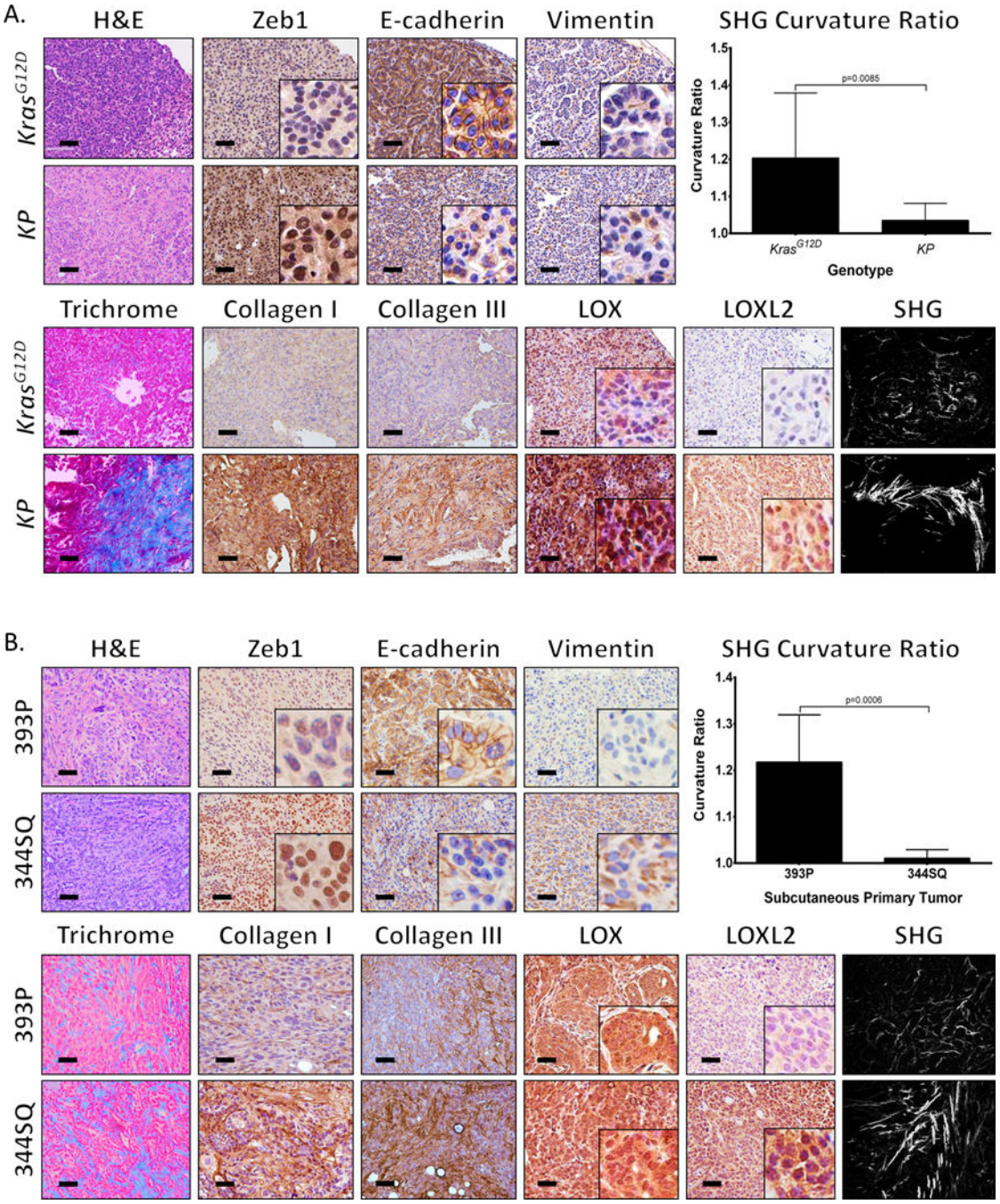

Figure 2. Metastatic lung tumors have increased collagen deposition and linearization

(A) Hematoxylin and eosin (H&E), Masson's trichrome, Zeb1, E-cadherin, Vimentin, collagen type I/type III, LOX, and LOXL2 immunohistochemical (IHC) stains, and second harmonics generation (SHG) microscopy of lung tumor tissues from non-metastatic $Kras^{G12D}$ and metastatic $Kras^{G12D};p53^{R172H}$ (KP) mice (n=5 tissues per group). **(B)** Staining of primary syngeneic tumor tissues generated by subcutaneous injection of non-metastatic 393P and metastatic 344SQ murine lung cancer cell lines in syngeneic mice (n=10 tumors per group). Upper right corners: Quantification of curvature ratio for

individual collagen fibers (n=50 collagen fibers per sample) imaged by SHG microscopy of tumor tissues from **(A)** and **(B)**. Microscopy images were captured at 20× magnification, scale bars represent 50 μm.

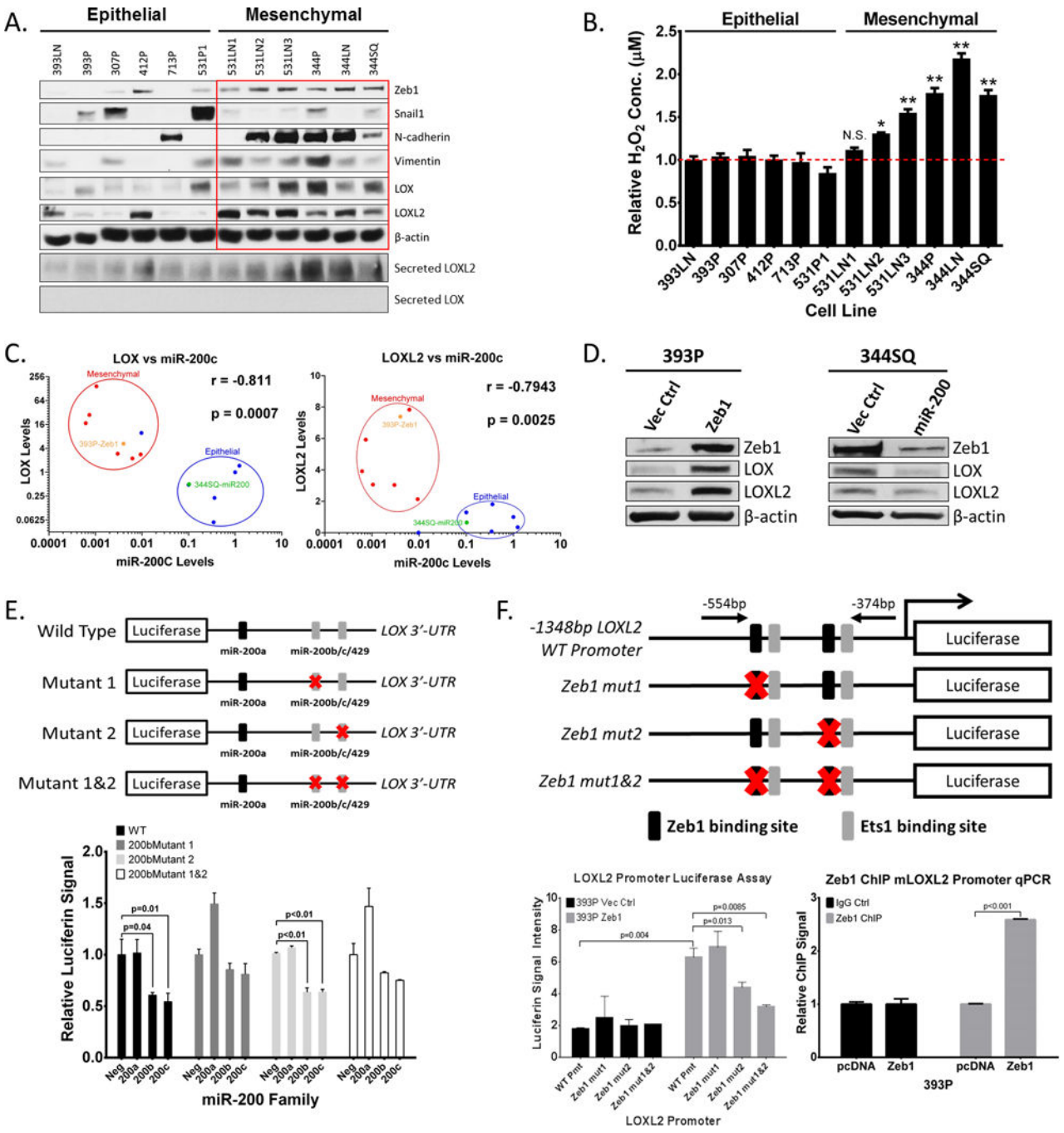

Figure 3. LOX and LOXL2 levels are higher in metastatic lung tumors and are directly regulated by miR-200 and Zeb1, respectively

(A) Top: Western blot analysis of Zeb1, Snail1, N-cadherin, Vimentin, LOX, LOXL2, and β-actin (loading control) in a panel of epithelial or mesenchymal murine KP lung cancer cell lines. Bottom: Western blot of secreted LOX and LOXL2 in conditioned media of murine panel cell lines. **(B)** Amplex Red assay to determine LOX/LOXL2 enzymatic activity in conditioned media of murine cell line panel. **(*)**: p<0.05 and **(**)**: p<0.01. **(C)** Cluster plots of normalized miR-200c and LOX or LOXL2 mRNA levels in epithelial and mesenchymal

murine lung cancer cell lines. 393P-Zeb1 and 344SQ-miR200 cells have also been included in the analysis. Data points represent mean ± SD (n = 3 samples). Spearman's rank correlation used for co-expression analysis. **(D)** Western blot analysis of Zeb1, LOX, LOXL2, and β-actin in epithelial 393P and mesenchymal 344SQ cell lines with constitutive Zeb1 or miR-200a/b/429 expression, respectively. **(E)** Top: Schematic of luciferase reporter constructs for wild-type (WT) mouse LOX-3′UTR and mutated potential miR-200b/c binding sites. Bottom: Relative luciferase activity of LOX-3′UTR reporter constructs above, co-transfected with non-targeting control miRNA, miR-200a, miR-200b, or miR-200c precursors in 344SQ cells. Three experimental replicates were performed with three technical replicates per experiment. **(F)** Top: Schematic of luciferase reporter constructs for mouse LOXL2 promoter region containing predicted Zeb1 and Ets1 binding sites. Mutations of potential Zeb1 binding sites indicated with red X and location of qPCR primers to amplify the region containing potential Zeb1 binding sites indicated by black arrows. Bottom-Left: Relative luciferase activity of LOXL2 reporter constructs above transfected into epithelial 393P cells with vector control or Zeb1 expression. Bottom-Right: Fold enrichment by qPCR analysis of LOXL2 promoter segments containing potential Zeb1 binding sites after chromatin immunoprecipitation in 393P-pcDNA vector control and 393P-Zeb1 cells, using Zeb1 antibody or mock IgG control antibody.

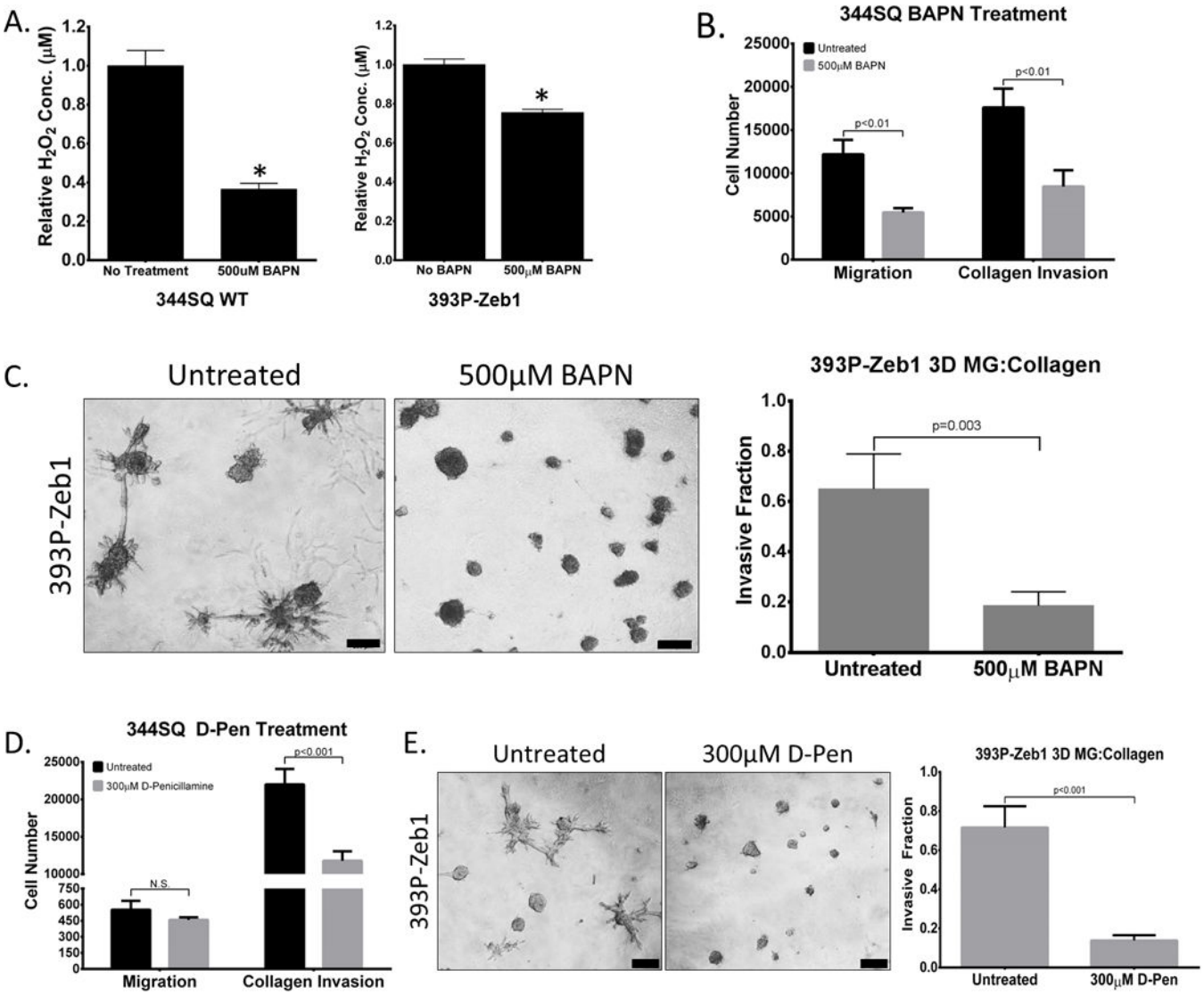

Figure 4. LOX enzymatic function is necessary for lung cancer cell migration and invasion

(A) Amplex Red assay to determine LOX/LOXL2 enzymatic activity in conditioned media of 344SQ and 393P-Zeb1 cells with or without 500 μM BAPN treatment. **(B)** Transwell migration and invasion through collagen for 344SQ cells treated with 500 μM BAPN. **(C)** 393P cells with constitutive Zeb1 expression cultured in a 3D matrix consisting of 1.5 mg/ml collagen/Matrigel mixture for 7 days, treated with 500 μM BAPN. **(D)** Transwell migration and invasion through collagen for 344SQ cells treated with 300 μM D-Penicillamine (D-Pen). **(E)** 393P cells with constitutive Zeb1 expression cultured in a 3D matrix consisting of 1.5 mg/ml collagen/Matrigel mixture for 7 days, treated with 300 μM D-Pen. Quantification of fraction of invasive structures in 3D culture assays to the right (n = 50 structures counted per condition). Microscopy images were captured at 4× magnification, scale bars represent 200 μm.

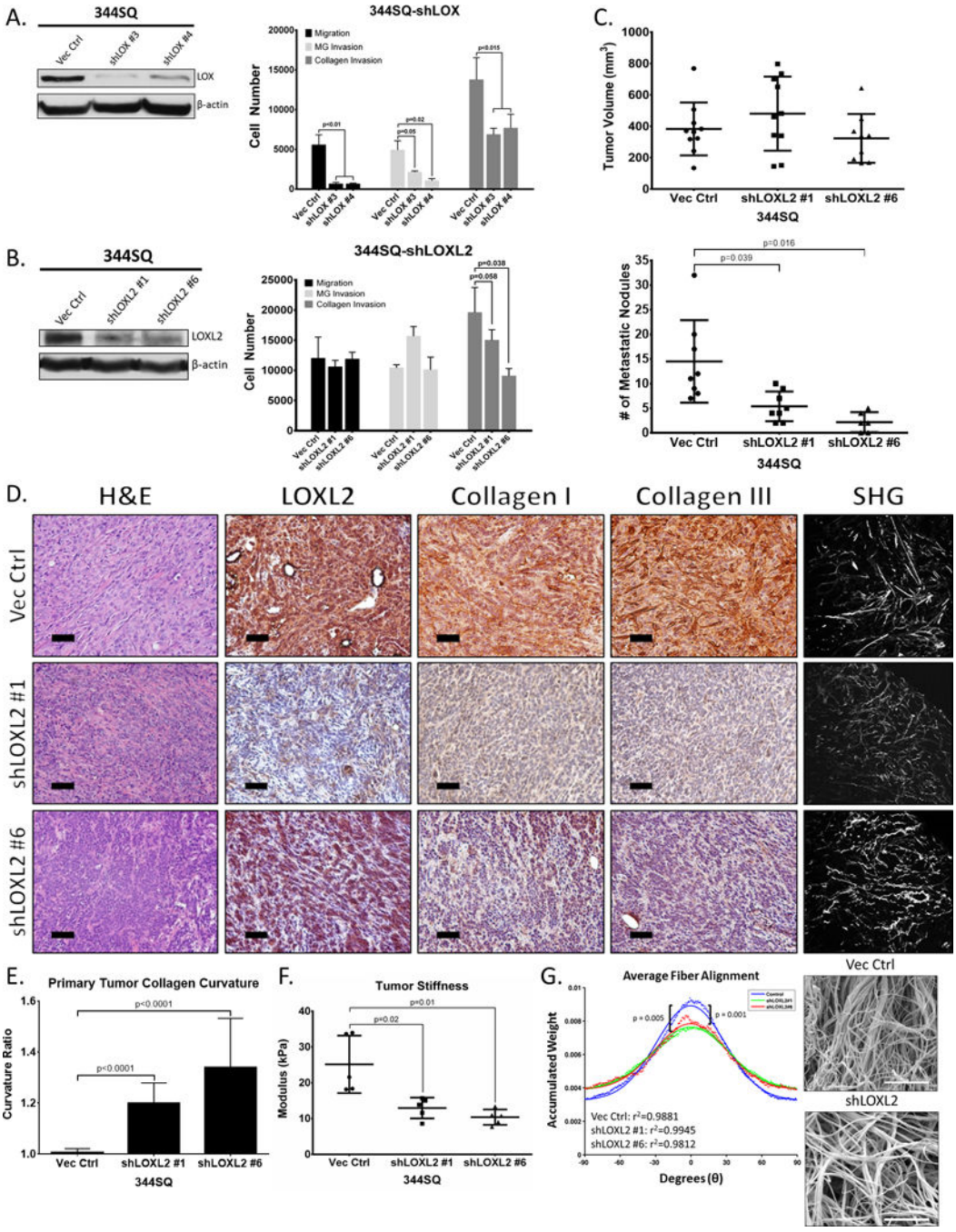

Figure 5. LOXL2 is necessary for collagen deposition, crosslinking and tumor cell metastasis

(A) Left: Western blot of LOX protein levels after stable shRNA knockdown in 344SQ cells. Right: Transwell migration and invasion through Matrigel and collagen for 344SQ cells with LOX knockdown. **(B)** Left: Western blot of LOXL2 protein levels after stable shRNA knockdown in 344SQ cells. Right: Transwell migration and invasion through Matrigel and collagen for 344SQ cells with LOXL2 knockdown. **(C)** Top: Primary subcutaneous tumor volume of 344SQ cells with stable LOXL2 knockdown injected in syngeneic wild type mice. Bottom: Quantification of lung metastatic surface nodules after subcutaneous injection of

344SQ cells with stable LOXL2 knockdown in syngeneic wild type mice. **(D)** H&E and IHC stains of LOXL2, collagen type I, and type III along with SHG microscopy of primary syngeneic tumor tissues from 344SQ cells with either a vector control or stable LOXL2 knockdown. Microscopy images were captured at 20× magnification, scale bars represent 50 μm. **(E)** Quantification of curvature ratio for individual collagen fibers imaged by SHG microscopy of tumor tissues from **(D). (F)** Mechanical stiffness measurements of tumor tissues from in D and E. **(G)** Right: Scanning electron microscopy (SEM) images of 2 mg/ml collagen gels after culturing 344SQ cells with or without LOXL2 knockdown. Images were viewed at 10kV and images were captured at 10kX magnification. Scale bars, 5 μm (n = 3 collagen gel molds per cell line). Left: Alignment analysis of collagen fibers to determine linearity and organization of collagen fibers as described in Methods section. The Kuiper test was used to test for differences in alignment between the sets of decimated data with significance as indicated.

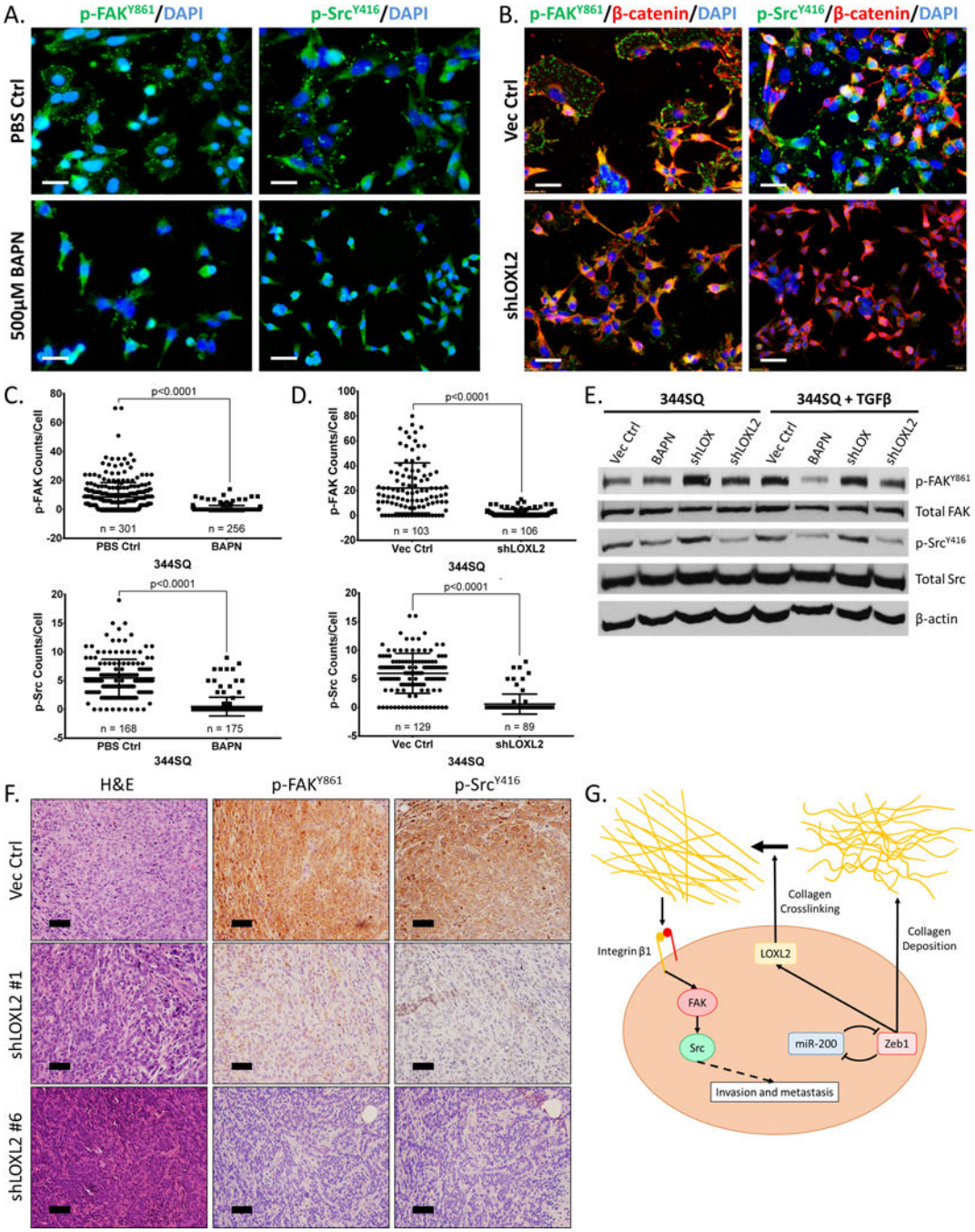

Figure 6. LOXL2-mediated collagen deposition induces FAK/Src signaling *in vitro* and *in vivo*

(A) Immunofluorescent staining of p-FAK^{Y861} and p-Src^{Y416} (green dots) in 344SQ cells treated with 5 ng/ml TGF-β for 48 hours in the presence or absence of 500 μM BAPN. **(B)** Immunofluorescent staining of p-FAK^{Y861}, p-Src^{Y416} (green dots), and β-catenin (red) in 344SQ cells after stable shRNA knockdown of LOXL2. β-catenin used as a marker to identify cell membrane. **(C)** Quantification of p-FAK^{Y861} and p-Src^{Y416} signal per cell from immunofluorescent stains in **(A). (D)** Quantification of p-FAK^{Y861} and p-Src^{Y416} signal per cell from immunofluorescent stains in **(B). (E)** Western blot of p-FAK^{Y861}, total FAK, p-

Src^{Y416}, and total Src in 344SQ cells ± 5 ng/ml TGF-β treatment for 48 hours in the presence of 500 μM BAPN, with stable LOX or LOXL2 knockdown. **(F)** H&E and IHC stains of p-FAK^{Y861} and p-Src^{Y416} of primary tumor tissues from subcutaneous injection of 344SQ cells with stable LOXL2 knockdown in syngeneic wild type mice. Microscopy images captured at 20× magnification, scale bars represent 50 μm. **(G)** Proposed model demonstrating Zeb1 regulation of collagen deposition in the tumor microenvironment through LOXL2 crosslinking and stabilization, activating the Integrin β1/FAK/Src signaling pathway in an autocrine manner leading to invasion and metastasis.

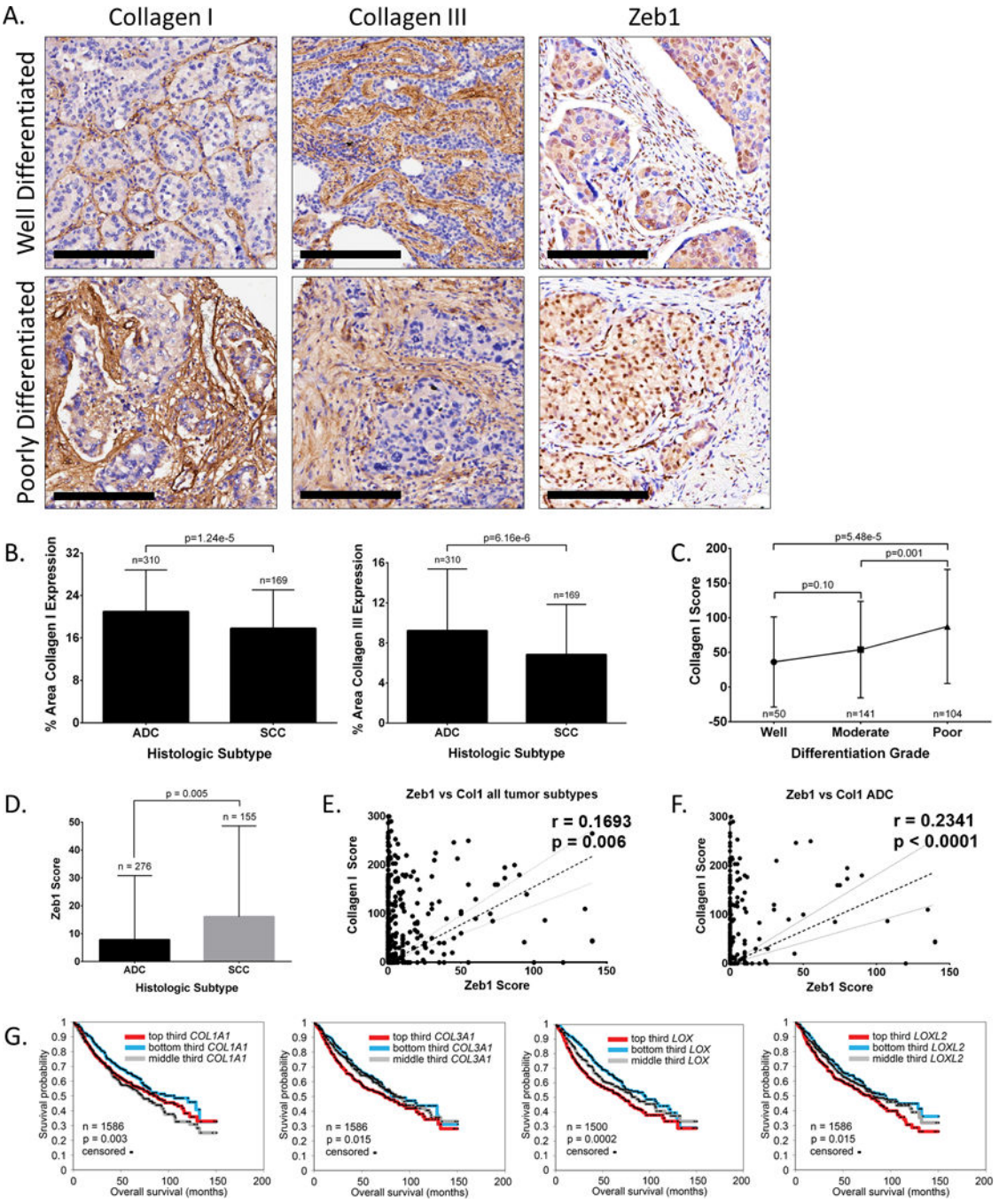

Figure 7. Increased collagen, LOX, and LOXL2 expression predicts poor prognosis among patients with lung adenocarcinoma

(A) Well differentiated and poorly differentiated human lung adenocarcinoma tissue sections IHC stained for collagen type I, collagen type III, and Zeb1. Scale bars, 200 μm. **(B)** Percent stromal area of tumor tissues with collagen type I or type III expression in patients with lung adenocarcinoma (ACC) or squamous cell carcinoma (SCC). **(C)** Average final cytoplasmic H-score of collagen type I expression in lung adenocarcinomas of different grades. **(D)** Average final nuclear H-score of Zeb1 in tumor cells of ADC or SCC specimens. **(E)** Cluster

plot analysis of Spearman's rank correlation between Zeb1 and collagen I H-score in both ADC and SCC specimens. **(F)** Cluster plot analysis of Spearman's rank correlation between Zeb1 and collagen I H-score in ADC samples. **(G)** Kaplan-Meier survival analysis by log-rank significance test of COL1A1, COL3A1, LOX, and LOXL2 mRNA expression levels versus overall lung cancer patient survival from a compendium expression dataset of 1,586 lung adenocarcinoma cases. P-values by log-rank test.